Total Synthesis and Bioactivity Mapping of Geodiamolide H

Veselin Nasufović,[a] Florian Küllmer,[a] Johanna Bößneck,[a] Hans-Martin Dahse,[b] Helmar Görls,[c] Peter Bellstedt,[d] Pierre Stallforth,[b] and Hans-Dieter Arndt*[a]

Abstract: The first total synthesis of the actin-stabilizing marine natural product geodiamolide H was achieved. Solid-phase based peptide assembly paired with scalable stereoselective syntheses of polyketide building blocks and an optimized esterification set the stage for investigating the key ring-closing metathesis. Geodiamolide H and synthetic analogues were characterized for their toxicity and for antiproliferative effects *in cellulo*, by characterising actin polymerization induction *in vitro*, and by docking on the F-actin target and property computation *in silico*, for a better understanding of structure-activity relationships (SAR). A non-natural analogue of geodiamolide H was discovered to be most potent in the series, suggesting significant potential for tool compound design.

Introduction

The geodiamolides are a collection of very closely related cyclodepsipeptide natural products isolated from marine *Geodia* sponges of the Caribbean sea. Geodiamolide H (**1**) and I (**2**) were isolated in 1998 from *Geodia corticostyliferia*, collected near the island of Barbados (Figure 1).[1] For both compounds, considerable anticancer potential was derived from their remarkable and selective cytotoxic activity against a panel of cancer-derived cell lines when compared with non-tumorigenic epithelial cells. Structurally, **1** and **2** are 19-membered ring macrolactones that feature a β-Tyr residue as the C-terminal amino acid. They display high similarity to the better-known jasplakinolide (**3**, JASP)[2] from which they only differ by a Trp→Tyr exchange for the second residue. All other geodiamolides (A-G, J-T) are 18-membered ring macrolactones that contain an aliphatic α-amino acid as the C-terminal residue, along with variations in the halogenation **X** of Tyr and the aliphatic amino acid residue (Gly or Ala, see Supporting Information, Figure S1).

The biosynthesis of geodiamolides has not been studied in detail. However, due to their high similarity to myxobacterial chondramides, they are likely produced by symbiotic bacteria of the *Geodia* sponges via related PKS/NRPS machinery.[3,4]

The geodiamolides bind and stabilize actin fibers (F-actin), thereby influencing cellular functions that are mainly connected to cell movement and transport.[5] Rules in substitution patterns can be derived from the structural motifs of isolated actin stabilizing macrocycles.[6–9] The stereochemistry of the polyke-

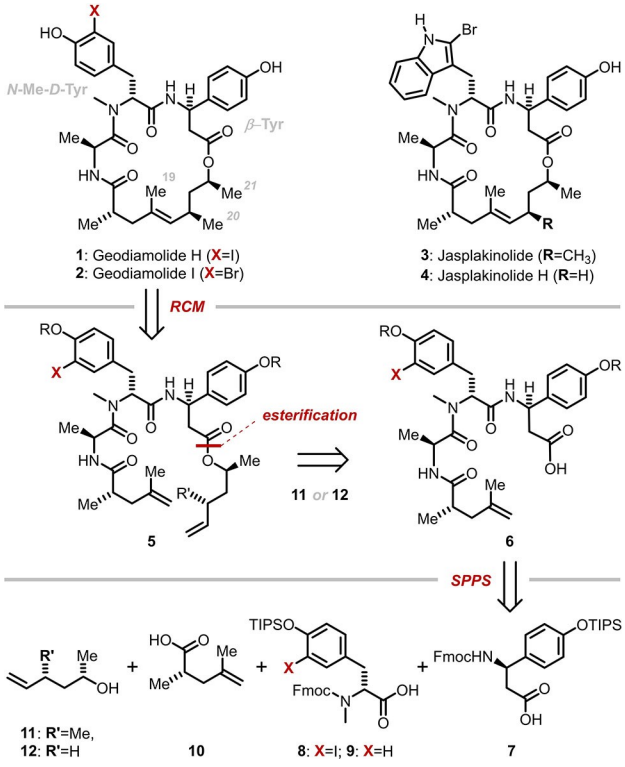

Figure 1. Cytotoxic F-actin-binding natural products and retrosynthetic simplification of 19-membered cyclodepsipeptides. Key positions of the geodiamolide H structure are indicated. Complete numbering can be found in the Supporting Information (Table S1).

[a] *V. Nasufović, Dr. F. Küllmer, J. Bößneck, Prof. Dr. H.-D. Arndt*
Institut für Organische Chemie und Makromolekulare Chemie
Friedrich-Schiller-Universität (FSU), Humboldtstr. 10, 07743 Jena (Germany)
E-mail: hd.arndt@uni-jena.de

[b] *Dr. H.-M. Dahse, Dr. P. Stallforth*
Abteilungen Infektionsbiologie und Paläobiotechnologie
Leibniz-Institut für Naturstoffforschung – Hans-Knöll-Institut
Beutenbergstr. 11a, 07745 Jena (Germany)

[c] *Dr. H. Görls*
Institut für Anorganische und Analytische Chemie
Friedrich-Schiller-Universität (FSU), Humboldtstr. 8, 07743 Jena (Germany)

[d] *Dr. P. Bellstedt*
NMR-Plattform, Friedrich-Schiller-Universität (FSU)
Humboldtstr. 10, 07743 Jena (Germany)

Supporting information for this article is available on the WWW under https://doi.org/10.1002/chem.202100989

tide stretch of the macrocycle is highly conserved throughout the family of natural products, whereas the tripeptide displays some variations whilst keeping affinity for the F-actin target.[10]

The actin-binding natural products phalloidin and jasplakinolide (**3**) played an essential role in studying actin-related processes and the F-actin structure itself, and are a relevant source of tool compounds.[11–16] Jasplakinolide is cell-permeable, and fluorescently labelled derivatives found broad applications.[14,17] However, F-actin-stabilizing molecules as drugs, e.g., for cancer therapy as "migrastatics",[18] have been difficult to develop due to their non-specific toxicity and potential absorption to abundant F-actin in muscles and vital organs. For further analyses, reliable and scalable syntheses of candidate molecules are necessary, as well as biological profiling and structure-activity relationship (SAR) data for mapping the accessible structure-function space.[18–21]

Although 19 geodiamolides have been described, only syntheses of geodiamolides A, B, and D have been reported to date.[22–24] However, very promising data regarding activity in 2D and 3D cancer models has been obtained in particular for geodiamolide H,[25,26] making this compound a highly interesting target for synthesis. Herein, we report the first total synthesis of geodiamolide H by streamlining our synthesis platform for F-actin-stabilizing ligands. We have furthermore synthesized and investigated simplified analogues of geodiamolide H, in order to locate key structural motives in compound SAR, in comparison to jasplakinolide and jasplakinolide H.[27]

Results and Discussion

Building block synthesis and assembly

In synthesis planning (Figure 1, bottom), geodiamolide H was simplified by a ring-closing metathesis to diene **5** that can easily be accessed from peptide acids **11** or **12** by esterification with an appropriate alcohol.[10,28,29] These peptides should be swiftly accessible by solid-phase peptide synthesis (SPPS) from the respective building blocks **7**–**12** (Figure 1). Syntheses of compounds **10** and **7** have been reported.[10] However, the previously described synthesis of alcohol **11**, harbouring the stereogenic methyl groups C-20 and C-21 (geodiamolide H numbering, Figure 1), featured a cumbersome alkylation of propanoylated pseudoephedrine auxiliary with propylene oxide, providing only 600 mg of product per 10 g of pseudoephedrine.[10] Moderate diastereoselectivity (84% *d.r.*) and access restrictions to pseudoephedrine were further reasons for developing an alternative route.

Our initial attempts of synthesizing alcohol **11** by alkylation of propanoylated prolinol and propanoylated Evans'-type auxiliaries remained unsuccessful, despite a screening of different electrophiles (Supporting Information, Scheme S1).[30–32] Enolates of Evans'-like imides are known to be only moderately reactive.[33] To circumvent sterically encumbered, weakly reactive electrophiles (Supporting Information, Scheme S1), we investigated Evans-like imide **15**, which upon methylation would provide the envisioned 1,3-dimethyl substituted building block by predictable auxiliary control (Scheme 1). A stereochemical mismatch, such as described earlier for chiral electrophiles,[10] cannot result from this planning.

Imide **15** was synthesized starting from (*S*)-propylene oxide, which was opened using allylmagnesium bromide to give alcohol **12** (84% yield).[34] TIPS protection, dihydroxylation, and oxidative cleavage of alcohol **12** produced aldehyde **14** in 64% yield (3 steps). $PhI(OAc)_2$-mediated oxidative esterification in the presence of *N*-hydroxysuccinimide[35,36] gave the respective O-Su ester (**14**–**1**) in 73% yield, which was used to acylate Seebach's diphenyl oxazolidinone to provide the desired imide **15** in 83% yield (Scheme 1).

Deprotonation of imide **15** with LDA is expected to produce a (*Z*)-configured lithium enolate rigidified by chelation.[33] Gratifyingly, treatment of the such obtained Li-enolate with MeI gave the branched imide **16** in excellent yield (89%) and diastereoselectivity (*d.r.* >99:1). This transformation was easily conducted on a larger (10 g) scale without any loss in yield or stereoselectivity. The configuration of imide **16** was unequivocally confirmed by single-crystal X-ray diffraction (Figure 2 and Supporting Information).

The primary alcohol **17** was liberated in excellent yield (98%) from imide **16** by treatment with $LiBH_4$. The Seebach auxiliary could be retrieved from this transformation for further use without chromatography by crystallization (70% recovery). Parikh–Doering oxidation of **17**, Wittig methylenation, and desilylation then gave the desired alcohol **11** in excellent yields each (83% over three steps).

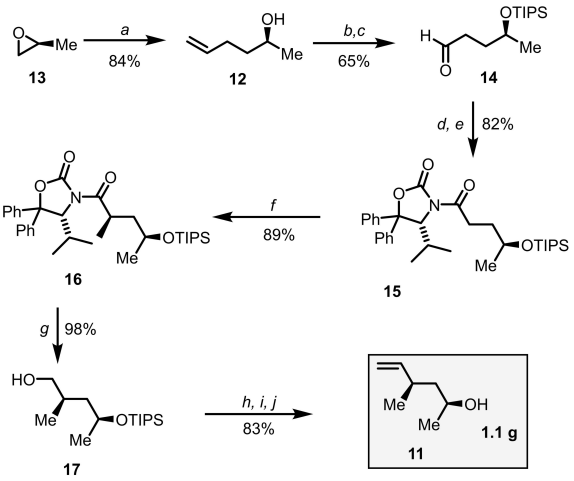

Scheme 1. Diastereoselective synthesis of (2*S*,4*R*)-4-methylhex-5-en-2-ol (**11**). Conditions and reagents: (a) Allylmagnesium bromide (1.3 equiv.), Et_2O, −78 °C, 2 h, 84%; (b) NaH (3.0 equiv.), TIPS-Cl (1.2 equiv.), THF, 0 °C to 25 °C, 16 h, 78%; (c) NMO (1.5 equiv.), 2,6-Lutidine (2 equiv.), OsO_4 (3 mol%), acetone/water (c = 0.1 M), 25 °C, 3 h, then $PhI(OAc)_2$ (1.5 equiv.), 3 h, 83%; (d) *N*-Hydroxysuccinimide (1.05 equiv.), 0 °C then $PhI(OAc)_2$ (1.05 equiv.), MeCN, −5 °C, 1 h, 73%; (e) Seebach's oxazolidinone (1.1 equiv.), *n*-BuLi (1.1 equiv., 2.35 M), THF, −78 °C, 10 min, then *active ester* from d (1.0 equiv.) in THF added, −78 °C to 25 °C, 16 h, 82%; (f) LDA (1.5 equiv.), THF, −78 °C 1 h, then MeI (12 equiv.), −40 °C, 4 h, 89%; (g) $LiBH_4$ (1.1 equiv.), H_2O (1.1 equiv.), THF, 0 °C, 3 h, 98%; (h) SO_3/Py (2.0 equiv.), DMSO (9 equiv.), DIPEA (4.0 equiv.), DCM -30 °C to 25 °C, 5 h, 94%; (i) *1i.* Ph_3PMeBr (2.2 equiv.), THF, −78 °C, BuLi (2.0 equiv.), 1 h then 30 min at 0 °C, *2i.* aldehyde from *h* (2.0 equiv.), −78 °C, 1 h, 92%, (j) TBAF (2.2 equiv.), THF, 25 °C, 6 h, 96%.

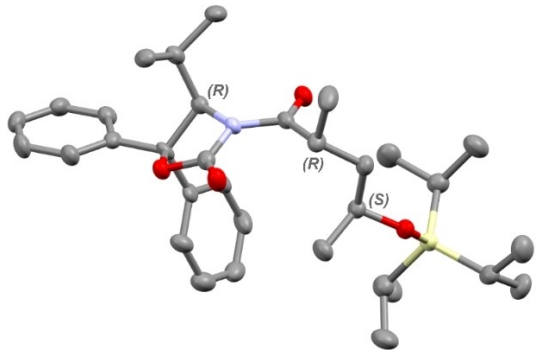

Figure 2. The solid-state structure of key intermediate **16** determined by single-crystal X-ray diffraction.

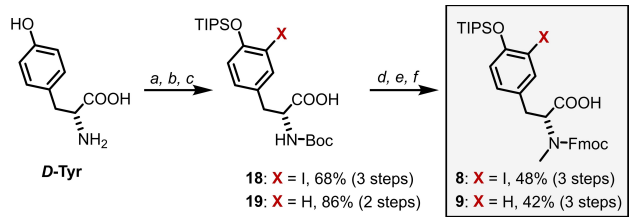

Scheme 2. Synthesis of *N*-Me-Tyrosine derivatives. Conditions and reagents: (a) I_2 in aq. NH_3 30% (1.0 equiv.), 0 °C, 3 h, 83% (only for synthesis of **8**); (b) Boc_2O (1.1 equiv.), TEA (1.5 equiv.), 1,4-dioxane/H_2O (1:1), 0 °C, 8 h, quant; (c) *1c.* DCE (1.05 equiv.) 0 °C, 30 min, DCM then TIPS-Cl (1.1 equiv.), 2 h, *2c.* Imidazole (2.0 equiv.), DMAP (0.2 equiv.), TIPS-Cl (1.1 equiv.), 16 h, 25 °C; *3c.* K_2CO_3 (2.0 equiv.), MeOH/THF/H_2O, 30 min, 25 °C; (d) NaH (2.1 equiv.), MeI (8.0 equiv.), THF, 0 °C to 25 °C, 16 h; (e) 20% TFA/DCM, 0 °C, 4 h, (f) Fmoc-OSu, 1,4-dioxane/H_2O, $NaHCO_3$, 0 °C to 25 °C, 16 h; for detailed procedures see Supporting Information.

The D-3-iodotyrosine building block **8** was synthesized by selective mono-iodination of D-tyrosine in an aqueous ammonia solution (Scheme 2).[37] Boc- and TIPS-protection delivered amino acid **18** in an overall yield of 68%. Double deprotonation of **18** with NaH, followed by alkylation with MeI and protection group exchange, provided the desired carbamate **8** for SPPS. The described route proved to be reliable as well for the synthesis of **9** (Scheme 2). Having these building blocks available, regular solid-phase peptide synthesis (SPPS) using 2-Cl-trityl chloride resin as solid support and COMU/Oxyma, as coupling reagents gave *N*-acylated tripeptides **21** and **22** in good yields, 77% and 84%, respectively.[38,39] HATU/HOAt as coupling reagent provided peptide **21** in 82% yield (see Supporting Information for details of SPPS).

Next, the esterification of peptide acids **21** and **22** was investigated. Esterification of amino acids and peptides with sterically demanding alcohol fragments can be problematic, especially when the availability of alcohol is limited or no excess can be used. Problems arise from the low nucleophilicity of the alcohol and the moderate reactivity of the activated carboxylic acid, which can undergo unwanted side reactions upon activation. Furthermore, the size of the activating reagent often additionally impairs reaction outcome.[40,41]

Efforts for establishing an efficient esterification under near-to stoichiometric conditions began by studying carbodiimide-mediated condensation under Steglich-type conditions (EDCI/DMAP).[42,43] Unfortunately, the reaction of tripeptide **21** (Table 1) with **12** (2 equiv.) gave only 22% of diene **25**. When alcohol **12** (1.3 equiv.) was reacted with **21** activated as acyl fluoride (TFFH),[44] as acyl chloride (Ghosez's reagent),[45] or with the MSNT reagent,[46] no product or minimal amount with

Table 1. Screening of esterification conditions and synthesis of linear ester-dienes.[a]

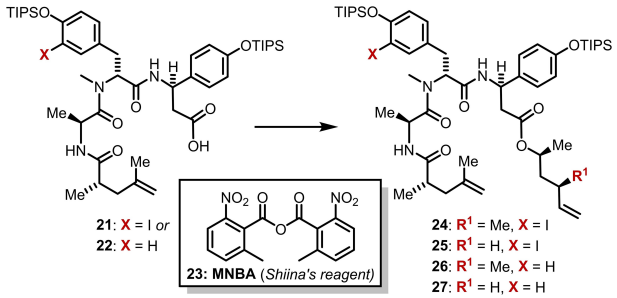

Entry	Peptide	Alcohol (equiv.)	Conditions (equiv.)		Product	Yield
1	21	12 *(2.0)*	*a*	EDCI *(1.0)*	25	22%
2	21	12 *(1.3)*	*b*	TFFH *(1.0)*	25	*n.c.*[b]
3	21	12 *(1.3)*	*c*	Ghosez's reag. *(2.0)*	25	*n.c.*[b]
4	21	12 *(1.3)*	*d*	MSNT *(2.0)*	25	<10%
5	21	12 *(1.3)*	*e*	Yamaguchi reag. *(1.0)*	25	46%
6	21	12 *(1.3)*	*f*	Shiina's reagent *(1.0)*	25	82%
7	21	11 *(1.3)*	*f*	Shiina's reagent *(1.0)*	24	74%
8	22	11 *(1.3)*	*f*	Shiina's reagent *(1.0)*	26	58%
9	22	12 *(1.3)*	*f*	Shiina's reagent *(1.0)*	27	77%

[a] Conditions and reagents: (a) EDCI, **12**, DMAP (0.2 equiv.), DCM 0 °C to 25 °C, 16 h; (b) TFFH, Et_3N (6.0 equiv.), DCM, 0 °C, 30 min at 25 °C then **12**, DMAP (0.2 equiv.), DCM 25 °C, 16 h; (c) Ghosez's reagent, DCM, 0 °C, 1 h, removal of volatiles, then: **12**, DMAP (0.2 equiv.), DCM 0 °C to 25 °C, 13 h; (d) MSNT, 1-Methylimidazole (2.0 equiv.), **12**, DCM, 0 °C to 25 °C, 16 h; (e) Yamaguchi reagent, THF, Et_3N (2.0 equiv.), 0 °C to 25 °C, 1 h, removal of volatiles, then: **12**, DMAP (1.2 equiv), toluene, 70 °C, 13 h; (f) Shiina's reagent, DIPEA (2.0 equiv), DCM, 25 °C, 30 min, then **11** or **12**, DMAP (1.0 equiv), DCM, reflux, 16 h. [b] *n.c.* = no conversion.

multiple side products was obtained. Notably, esterification by using the Yamaguchi reagent gave diene **25** in 46% yield.[47] Gratifyingly, by using the anhydride of 2-methyl-6-nitrobenzoic acid (MNBA, Shiina's reagent),[48] esters **24**–**27** were obtained in good yields (58–82%) using only a slight excess of alcohols **11** or **12** (1.3 equiv.), as a significant improvement compared to previous results.[10]

Ring closing metathesis

Ring-closing metathesis has been used before as a key macrocyclization step for the synthesis of jasplakinolide-type cyclodpesipeptides.[10,28,49] For the synthesis of the geodiamolides, large amounts of Grubbs 2nd generation catalyst **28** (35 mol%) in toluene had to be used with a constant purge of argon, in order to cyclize diene **24** to an almost equimolar mixture of configurational isomers ***E*-29/*Z*-30** in moderate yield (53% combined, Table 2) that was difficult to quantify exactly due to impurities. At lower catalyst loadings, conversion dropped strongly, in line with earlier findings for jasplakinolide-like polyketide segments.[10,49] Simultaneous TIPS deprotection by using 30% HF/pyridine, followed by separation of the alkene isomers by prep. HPLC gave the *E*-configured natural product geodiamolide H, as well as the non-naturally *Z*-configured geodiamolide H isomer **35**, both in good yield (42% and 36%, Table 2). Configurations of the final products were assigned by selective 1D NOE experiments. Spectral properties of synthetic **1** matched the data of isolated material (Supporting Information, Table S1),[1] thus indicating completion of the total synthesis of geodiamolide H.

Likewise, processing of the halogen-free diene **26** resulted in a similar outcome, again giving a mixture of configurational isomers ***E*-32** and ***Z*-33** (Table 2) in almost equal amounts. The diene precursors **25** and **27**, each devoid of the allylic C-20 methyl group, cyclized much more efficiently. Macrocycles **31** and **34** were obtained by using only 7 mol% of the catalyst over 2 h, exclusively as *E*-isomers, as confirmed by selective 1D NOE experiments. Deprotection of TIPS groups and HPLC purification provided the geodiamolide analogues **35**–**39** in very good yield (Table 2).

The strong variation in yields, stereoselectivity, and turnover observed for the different macrocyclization reactions prompted a more detailed study. Alkene metathesis may be kinetically or thermodynamically controlled, depending on the kinetics of individual steps.[50] As a general rule, the rate of Ru-carbene-mediated metathesis significantly drops with the increased steric encumbrance of the alkene substrates, and with their electron deficiency.[51] For jasplakinolide-type macrocycles, previous data had suggested that ring closure and *E*/*Z* ratio are kinetically controlled.[49] However, in the case of diene **24**, which showed particularly retarded turnover, a major side product was isolated in 25% yield, accounting for the bulk of the missing mass balance. This side product was indistinguishable from starting diene **24** in HPLC retention time, TLC R_f value, and exact mass (HRMS/TOF). Careful monitoring by NMR revealed the disappearance and shift of one vinylic proton (Supporting Information, Figure S2 and S3), indicative of an isomerization of the terminal double bond to the even less reactive trisubstituted alkene isomers **40** (Scheme 3). Olefin isomerization during metathesis using Ru catalysts has been described before and has been attributed to catalyst decomposition and/or the presence of Ru hydride intermediates.[52,53] In the case of dienes **25** and **27**, a comparable isomerization was not observed. These reactions proceeded stereoselectively to full conversion in a much shorter time (Scheme 3, ***E*-31**). The substitution pattern bearing an allylic methyl group (in case of **24** and **26**) is apparently more prone to isomerization or catalyst decomposition, likely due to delayed turnover by steric encumbrance of the macrocyclization's transition state. Supporting this notion, adding benzoquinone to the mixture for suppressing catalyst to suppress the formation of Ru hydride intermediates, as described,[54] did not change the result, indicating a substrate mediated side reaction, leading to catalyst degradation. This

Table 2. Macrocyclization and completion of synthesis.[a]

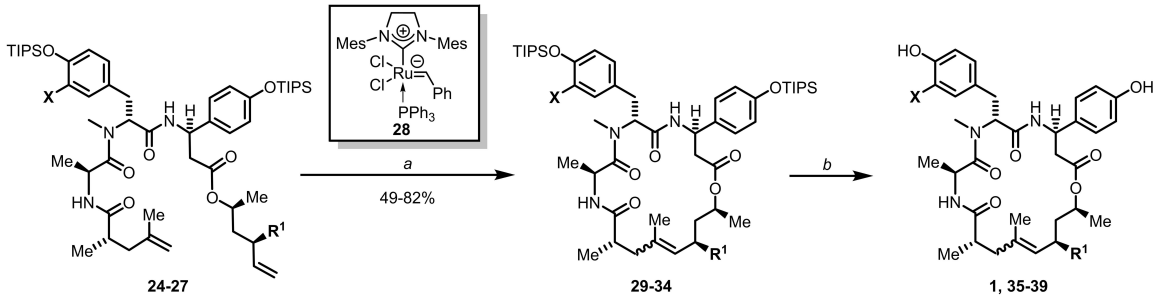

Entry	Diene	X	R^1	RCM products (yield)	Final products (yield)
1	**24**	I	Me	***E*-29/*Z*-30** (53%)[b]	***E*-1** (42%)[c] and ***Z*-35** (36%)[c]
2	**25**	I	H	***E*-31** (74%)[c]	***E*-36** (74%)[c]
3	**26**	H	Me	***E*-32/*Z*-33** (49%)[b]	***E*-37** (39%)[c] and ***Z*-38** (32%)[c]
4	**27**	H	H	***E*-34** (82%)[c]	***E*-39** (84%)[c]

[a] Conditions and reagents: (a) Grubbs catalyst 2nd generation **28** (7 mol% for **25** and **27**, 35 mol% for **24** and **26**), toluene, 0.1 mM concentration, reflux with constant purge of Ar, 2 h (for **25** and **27**), 4 h (for **24** and **26**); (b) 70% HF/Pyridine, THF, 25 °C, 24 h, N_2, prep. HPLC. [b] Combined, roughly equimolar *E*/*Z*-ratio as estimated by ^{1}H NMR spectroscopy. [c] Isolated yield after purification.

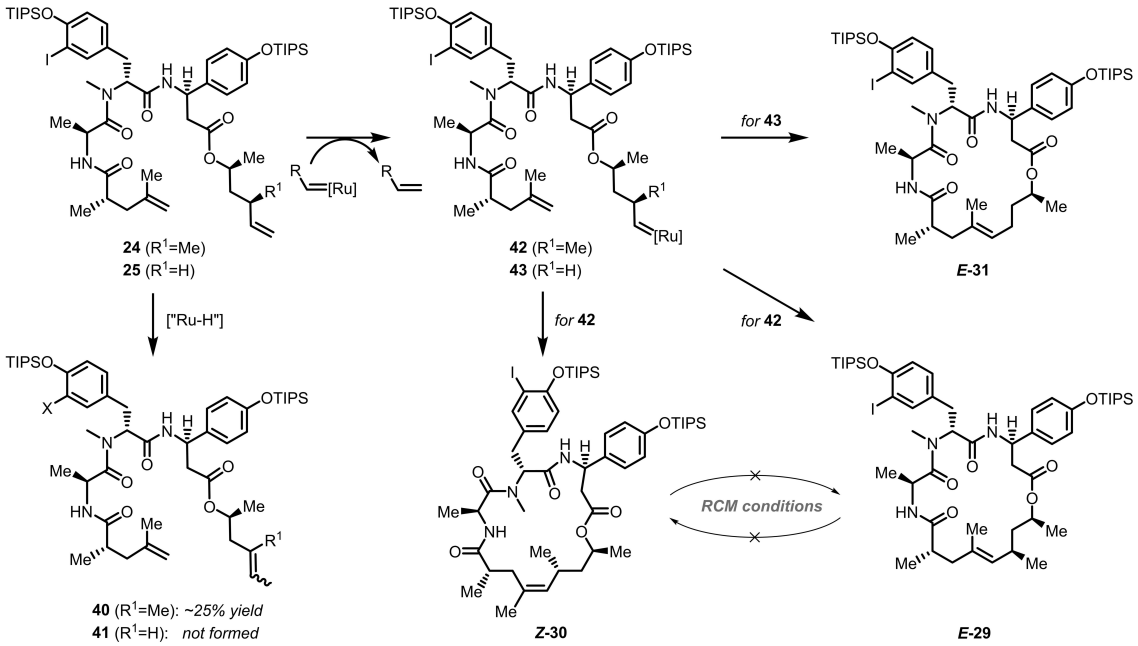

Scheme 3. Competitive pathways of product formation during ring-closing metathesis.

qualitatively accounts for the elevated amounts of catalyst needed in this case. It may be speculated that Ru methylene complexes are involved, as active purging of the mixture with Ar in order to remove traces of ethylene was found indispensable to observe reasonable product formation.

For further insight, the *bis*-TIPS protected macrocycles ***E*-29** and ***Z*-30** were separated and independently studied (Scheme 3). Repeated exposure of ***E*-29** and ***Z*-30** to the reaction conditions with NMR monitoring suggested that these compounds were completely stable to treatment with Grubs 2nd generation catalyst. Neither isomerization nor ring fission or polymerization were observed, suggesting that both geometrical isomers are independently formed during initial ring closure (Supporting Information, Figure S4). Variation of catalyst amount or reaction time did not produce different results. Collectively, the available data strongly suggests that these macrocyclization reactions are fully under kinetic control, and that the observed, substrate-dependent *E*/*Z* ratios are a result of RCM intermediate conformer accessibility.

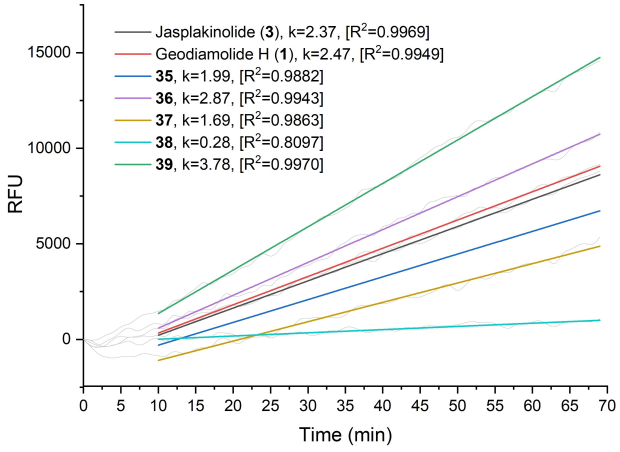

Figure 3. *In vitro* actin polymerization induced by cyclodepsipeptides. *Geodiamolides* and *jasplakinolide* (each 20 μM) were incubated with pyrene-labelled actin (5 μM) under low salt non-polymerizing conditions. *k*: slopes of linearly fitted curves given in RFU/s; see Supporting Information for details.

Biological activity on target

We then turned our attention to the biological activity of the geodiamolides. To assess the potency of the geodiamolides on target, we studied actin polymerization induction *in vitro* in comparison to jasplakinolide (Figure 3, Table 3). We compared the apparent polymerization rates that were normalized to jasplakinolide at a similar concentration (K_{rel}, see Supporting Information for details).[17] Geodiamolide performs as strongly as jasplakinolide H (K_{rel} = 1.04, Figure 3, Table 3). The unnatural *Z*-isomer of geodiamolide H (**35**) shows slightly reduced potency (K_{rel} = 0.84), but is still significantly inducing polymerization, as is the *E*-configured des-iodo-geodiamolide H analogue **37** (K_{rel} = 0.71).

However, for the *Z*-configured des-iodo-analogue **38** a significant drop in activity was found (K_{rel} = 0.12), suggesting that olefin geometry and tyrosine halogenation are synergistic. As suggested before, the olefin in the polyketide might serve as a hinge for the positioning of the tripeptide towards the F-actin target.[10]

Des-methyl geodiamolide H **36** showed high activity *in vitro* (K_{rel} = 1.21), but even higher activity is found for the des-methyl-des-iodo analogue **39** (K_{rel} = 1.59). Jasplakinolide analogues

devoid of the C-20 methyl group have been previously found to be equally cytotoxic to jasplakinolide.[10] What surprises is the elevated activity of the dehalogenated compound **39**, which may be attributed to the higher flexibility of des-methyl analogues that suffer less from *syn*-pentane interactions (C20 ↔C21) or allylic strain (C19↔C20, jasplakinolide numbering). Apparently, ligand binding appreciably benefits from the higher conformational flexibility of the macrocycles **36** and **39**. This flexibility is also indicated by ^{1}H NMR data of the simplified analogue **39** that showed more than one conformational population in solution (see Supporting Information).

Cytotoxicity

Prolonged blocking of cytoskeletal dynamics by small molecules leads to cellular toxicity. Synthetic geodiamolide H and its variants were hence subjected to methylene blue assays with HeLa cell cultures to estimate their general cytotoxicity, using jasplakinolide (**1**) as control.[55] Geodiamolide H shows a CC_{50} of 410 nM in HeLa cells, comparable to the results reported by the isolation group for a different cell line.[1] Interestingly, the *in cellulo* cytotoxicity data did mirror the results on induction of F-actin polymerization *in vitro* only loosely (Table 3). The *Z*-isomer of geodiamolide H **35** was one order of magnitude less cytotoxic than **1**, which was also found for the activity of the geometrical isomers of jasplakinolide.[56] The highest toxicity was observed for the des-methyl analogue **36** (130 nM), comparable to jasplakinolide (81 nM). However, the compound most active *in vitro*, geodiamolide analogue **39**, displayed only modest toxicity (2.3 μM). We speculate that differential cell permeability of the macrocycle may be the reason for this difference, as this property may be dependent on substitution pattern and even conformation. However, other factors such as compound stability and/or solubility differences may be involved, too.[57]

To study antiproliferative effects, we have tested geodiamolide H and analogues were tested using human umbilical vein endothelial cells HUVEC (ATCC CRL-1730) and human chronic myeloid leukaemia cells K-562 (DSM ACC 10). All compounds, except for **38**, show high activity (GI_{50}) toward HUVEC cells. Similar to the toxicity pattern in the HeLa cell line, the simplified analogue **36** showed higher activity than jasplakinolide (**1**, Table 3).

Computational studies

In order to gain a deeper understanding of the *in vitro* and *in cellulo* SAR results, and to collect data for designing actin ligands with desired properties, *in silico* structural modelling was performed using the ExtraPrecision (XP) Docking Mode as implemented in the Glide software package (Schroedinger Inc).[58] Specifically, jasplakinolide-bound, aged F-actin was used as an input for ligand docking in its ligand-depleted form (PDB 6T23).[59] The docking procedure was verified by re-establishing the binding pose of jasplakinolide Q, which resulted in an *in silico* pose with <1.0 Å RMSD of all heavy atom positions (See Supporting Information). Docking of geodiamolide was performed similarly, leading to a pose with <1.6 Å RMSD when compared to jasplakinolide. While it cannot be excluded that the F-actin target structure may minimally adapt to the exchanged small molecule ligand,[60,62] this similarity is much higher than the experimental resolution of Cryo-EM (2.9–4 Å) and hence allowing SAR comparison.

To estimate binding affinity, a docking score was calculated for each geodiamolide ligand and for jasplakinolide, using the same ligand-depleted jasplakinolide-bound F-actin structure as an input.[59] The data obtained were congruent with the *in vitro* F-actin polymerization data, rendering simplified analogue **39** as the best binding compound, followed by natural products geodiamolide H and jasplakinolide (Table 4). The relative binding energies were also estimated based on the commonly employed MM-GBSA rescoring approach before and after short molecular dynamics simulations. We found, however, the XP docking score to be the parameter fitting best to the *in vitro* data for geodiamolide congeners (see Supporting Information, Table S2).[60,61]

As the cellular activity was neither in full agreement with the *in vitro* data nor with the docking scores, we also scrutinized *in silico* ADME data as available from the QikProp module of Schroedinger's Drug Discovery Suite. The aqueous solubility parameter such predicted (QPlogS, Table 4) correlated significantly with the observed *in cellulo* activity of geodiamolides and jasplakinolide. Furthermore, permeability by passive trans-

Table 3. Activity of geodiamolide H and analogues *in cellulo* and on target:[a]

Entry	Compound	R	X	E/Z	Cytotoxicity[ii] HeLa CC_{50}[μM]	Antiproliferative activity[ii] HUVEC GI_{50}[μM]	K-562 GI_{50}[μM]	Activity on target relative slope (RFU/s)[a]	K_{rel}[i]
1	**JASP (3)**			*E*	0.08 (±0.01)	0.010 (±0.002)	2.4 (±1.0)	2.37	1.00
2	**geod. H (1)**	CH_3	I	*E*	0.4 (±0.01)	0.27 (±0.08)	8.2 (±3.1)	2.47	1.04
3	**35**	CH_3	I	*Z*	6.5 (±0.3)	4.8 (±0.8)	14 (±2)	1.99	0.84
4	**36**	H	I	*E*	0.13 (±0.10)	0.008 (±0.001)	5.6 (±1.1)	2.87	1.21
5	**37**	CH_3	H	*E*	1.0 (±0.1)	1.0 (±0.1)	>82	1.69	0.71
6	**38**	CH_3	H	*Z*	78 (±4)	57 (±3)	48 (±5)	0.28	0.12
7	**39**	H	H	*E*	2.4 (±0.2)	1.7 (±0.3)	>84	3.78	1.59

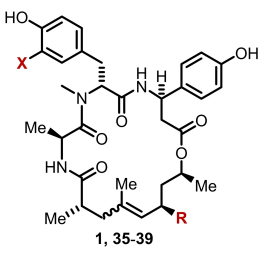

1, 35-39

[a] Comments: [i] K_{rel}-relative change in fluorescence intensity of pyrene-labelled actin over time relative to the same change induced by jasplakinolide (both in the linear part of the curve after applying linear fit); [ii] data rounded to meaningful digits.

Table 4. *In silico* calculated parameters for geodiamolide H and analogues:[a]

Entry	Compound	R	X	E/Z	In cellulo H_{rel}[i]	In vitro K_{rel}[ii]	In silico Binding docking score[iii]	ADME QPlogS[iv]	QPPMDCK[v]
1	**JASP (3)**			*E*	1	1	−6.13	−6.08	329.80
2	**geod. H (1)**	CH_3	I	*E*	0.2	1.04	−6.21	−5.11	189.31
3	**35**	CH_3	I	*Z*	0.01	0.84	−4.31	−4.26	171.01
4	**36**	H	I	*E*	0.62	1.21	−5.82	−5.88	227.66
5	**37**	CH_3	H	*E*	0.08	0.71	−5.50	−4.11	125.46
6	**38**	CH_3	H	*Z*	0.001	0.12	−5.20	−4.05	63.55
7	**39**	H	H	*E*	0.03	1.59	−7.12	−3.33	58.47

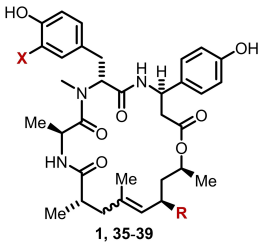

[a] Comments: [i] H_{rel}-relative cytotoxicity to jasplakinolide in HeLa cell line; [ii] K_{rel}-relative change in fluorescence intensity of pyrene-labelled actin over time relative to the same change induced by jasplakinolide (both in the linear part of the curve after applying linear fit); [iii] Docking score units are kcal/mol; [iv] Predicted aqueous solubility – log S; S (in mol dm^{-3}); [v] predicted apparent MDCK cell permeability (in nm/sec).

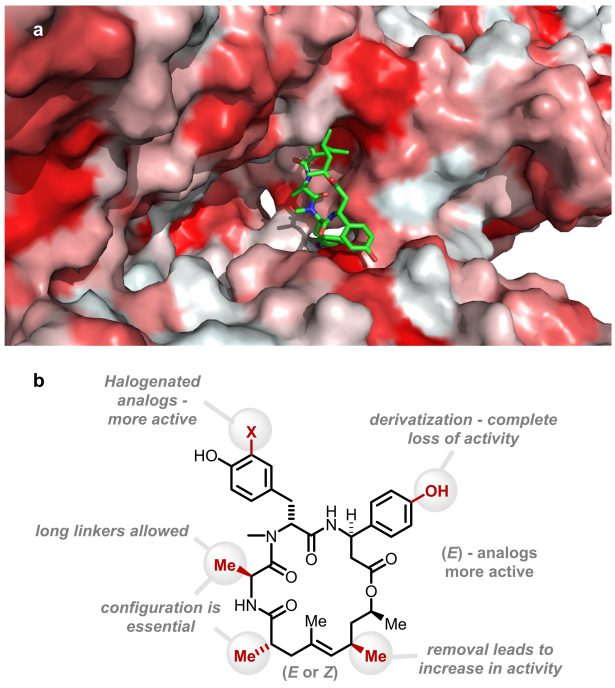

Figure 4. The binding site of cyclodepsipeptides on F-actin and SAR; (a) Geodiamolide H docked in the binding cleft of F-actin (PDB 6T23), amino acids on the surface of the protein are marked according to hydrophobicity;[62,68] (b) Compiled SAR features of geodiamolides.

port through MDCK cells was computed as well (QPPMDCK, Table 4). These *in silico* data rank the tested compounds accordingly, such as to suggest the most active compound *in vitro* (**39**, K_{rel} = 1.59) being the least permeable, congruent to its impaired activity in cellular models. By contrast, jasplakinolide, which induces F-actin polymerization similar to geodiamolide H, is predicted to be highly cell-permeable *in silico*, which could explain the high, acute toxicity of this natural product. While certainly being only a rough estimate, qualitatively, these data suggest that solubility and permeability may significantly change by halogenation status and polyketide methylation of the cyclodepsipeptide scaffold, contributing to overall compound activity and – possibly – cell-type specificity.[25,26]

On a structural level, recently reported cryo-EM structures of a polar jasplakinolide analogue[12] and of jasplakinolide and phalloidin bound to the F-actin fibre,[59,62,63] as well as of target-bound photoswitchable jasplakinolide derivatives (**optojasps**),[64,65] all show a highly similar orientation of the macrocycle in the binding region on F-actin. A very similar binding pose was found for geodiamolide H by docking (Figure 4a, and Supporting Information, Figures S7–S9). The signature tryptophan residue of jasplakinolides and of phalloidin is buried deeply inside a cleft present in F-actin, which in case of geodiamolide H (**1**) accommodates the iodo-tyrosine moiety. The amino acid residues on F-actin proximal to the β-tyrosine residue are highly hydrophobic (marked red in Figure 4a), as are these in the proximity of the polyketide. While these hydrophobic interactions seem to play the most significant role in ligand binding and F-actin fibre stabilization, and specific interactions were not experimentally resolved by cryo-EM, the docking procedure indicated key H-bonds of ligand backbone amides to F-actin (^{197}Gly, ^{199}Ser), and of the phenolic OH of iodotyrosine as well (^{110}Leu, see Supporting Information, Figure S10). Interestingly, the key iodotyrosine (geodiamolides) or indole residue (jasplakinolides, phalloidin) seems to benefit from a cation-π interaction with ^{177}Arg on F-actin,[66] qualitatively in line with the necessity for featuring a polarizable arene at this position.[67]

Conclusions

On the molecular level, jasplakinolide and the geodiamolides stabilize a protein-protein interaction,[69,70] a property recently generally also attributed to "molecular glues".[71] The SAR data of this study and of previous reports on similar compounds are summarized in Figure 4b.[10,56] Interestingly, while the removal of the C-20 methyl group from jasplakinolide is known to be tolerated,[10] for geodiamolide H it even leads to an increase in cytotoxicity. On the other hand, side chain dehalogenation leads to reduced cellular activity for geodiamolide H, but not for jasplakinolide. This feature is likely connected to modulated cellular permeability, as the activity on target was barely affected *in vitro*. Not tested in this study, but shown before on several examples, the L-alanine moiety may be extended by

long linkers and bulky substituents. F-Actin stabilizing cyclodepsipeptides with the "native" *E*-geometry of the double bond show higher toxicity. Since geodiamolides share the binding site with jasplakinolide, derivatization of the β-tyrosine phenol moiety can be expected to lead to inactive compounds.

In summary, we have developed a reliable synthesis of geodiamolide H and demonstrated its scope by the synthesis of a focussed set of geodiamolide H analogues. An improved stereoselective route for the synthesis of chiral alcohol **11** and an optimized esterification of tripeptides streamlined the synthesis of the jasplakinolide-type cyclodepsipeptides. The pitfalls of the key ring-closing metathesis for the macrocyclization were mended. These insights will be beneficial for the synthesis of other members of this natural product family, as well as for optimal synthesis design of chemical biology probes. All synthetic geodiamolide H analogues were tested *in cellulo* and *in vitro*, which allowed creating an initial SAR model. Additional *in silico* data supported compound solubility and cell permeability to be significantly modulated by structural modification. Collectively, these data should inspire the design of new chemical probes for studying actin function, assist in quantification of cellular functions, or become instrumental for actin targeting therapeutics.

Experimental Section

General

All general procedures, materials, methods, and abbreviations can be found in the Supporting Information.

Scalable procedure for peptide esterification

The peptide acid (0.1 mmol, 1 equiv.) was mixed with MNBA (0.1 mmol, 1 equiv.) and EtN(*i*-Pr)$_2$ (0.2 mmol, 2 equiv.) in CH_2Cl_2 (7 mL) at 25 °C and stirred for 30 min. DMAP (0.1 mmol, 1 equiv.) was added, followed by the addition of the corresponding alcohol (0.13 mmol, 1.3 equiv.). The mixture was heated to reflux for 16 h, cooled to 25 °C, diluted with CH_2Cl_2 (30 mL), and washed with water (10 mL). The organic layer was dehydrated (Na_2SO_4), the solvent was evaporated under reduced pressure, and the product was purified by flash column chromatography.

Scalable procedure for ring closing metathesis

Toluene (80 mL) was added to a two-neck flask, and degassed by heating to reflux and active purging with argon for 30 min. The linear diene precursor (0.1 mmol, 1 equiv.) was dissolved in a small amount of degassed CH_2Cl_2 and added to the degassed toluene. The solution was heated to reflux with a continuous purge of argon for 30 min, and Grubbs 2nd generation catalyst was added (6.2 mg, 7.5 mol% for (*S*)-hex-5-en-2-ol esters; 28.8 mg, 35 mol% for (*2S,4R*)-4-methylhex-5-en-2-ol esters). Refluxing was continued for several hours with a constant purge of argon and TLC monitoring. After conversion was complete, the solvent was evaporated under reduced pressure and the residue was purified by flash column chromatography.

Scalable procedure for final deprotection

The silylated macrocycle (0.1 mmol) was dissolved in THF (700 μL) in a 15 mL PP Falcon tube. 70% HF/pyridine complex (50 μL) was added and the mixture was stirred for 16 h at 25 °C under N_2. Volatiles were evaporated in a stream of N_2 under a ventilated hood. The residue was dissolved in 5 mL of CH_2Cl_2, passed through a pad of silica gel (1 cm), concentrated under reduced pressure, and purified using preparative HPLC.

Geodiamolide H

Final deprotection was conducted with a mixture of cyclodepsipeptides ***E*-29** and ***Z*-30** (16 mg). 4.7 mg of Geodiamolide H (**1**, 42% yield) and 3.9 mg (36% yield) of its unnatural *Z*-isomer ***Z*-35** were obtained after prep. HPLC, each as colourless solids.

***E*-Isomer** (Geodiamolide H, **1**): m.p. 137 °C, TLC R_f = 0.18 (hexanes/EtOAc = 3:7); $[\alpha]_D^{24}$ = +22.6 (c = 0.1, $CHCl_3$:MeOH = 1:1); IR (ATR): $\tilde{\nu}$ = 3014 (w), 2970 (w), 2922 (w), 2717 (w), 2607 (w), 2375 (w), 2311 (w), 2161 (w), 2106 (w), 1944 (w), 1868 (w), 1736 (m), 1654 (w), 1508 (m), 1457 (w), 1419 (w), 1364 (m), 1216 (m), 1132 (w), 1097 (w), 1025 (w), 901 (w), 816 (w), 669 (w), 615 (w) cm^{-1}; ^{1}H NMR (600 MHz, DMSO-d_6, 297 K): δ = 10.08 (s, 1H), 9.31 (s, 1H), 8.24 (d, *J* = 8.8 Hz, 1H), 7.72 (d, *J* = 7.7 Hz, 1H), 7.49 (d, *J* = 2.0 Hz, 1H), 7.06 (d, *J* = 8.5 Hz, 2H), 7.00 (dd, *J* = 8.3, 2.0 Hz, 1H), 6.72 (d, *J* = 8.2 Hz, 1H), 6.68 (d, *J* = 8.5 Hz, 2H), 5.30 (dd, *J* = 10.7, 5.5 Hz, 1H), 5.13 (d, *J* = 4.0 Hz, 1H), 4.82 (d, *J* = 8.5 Hz, 1H), 4.61 (dd, *J* = 14.1, 7.3 Hz, 2H), 2.94 (s, 3H), 2.88 – 2.72 (m, 2H), 2.70–2.52 (m, 4H), 2.29 (m, 2H), 2.18 – 2.10 (m, 1H), 1.82–1.73 (m, 1H), 1.68–1.54 (m, 1H), 1.52 (s, 3H), 1.32 – 1.22 (m, 1H), 1.06 (d, *J* = 6.2 Hz, 3H), 0.96 (d, *J* = 6.8 Hz, 3H), 0.84 (d, *J* = 6.6 Hz, 3H), 0.81 (d, *J* = 6.8 Hz, 3H) ppm; ^{13}C{^{1}H} NMR (125 MHz, DMSO-d_6, 297 K): δ = 174.0, 173.0, 169.9, 169.1, 166.5, 158.6, 156.4, 156.3, 155.4, 138.3, 132.8, 132.2, 131.5, 130.4, 129.9, 129.2, 127.0, 125.8, 115.1, 114.5, 113.6, 74.8, 70.4, 70.1, 63.8, 62.9, 55.0, 54.9, 48.5, 44.1, 43.6, 42.9, 41.6, 38.2, 37.2, 33.3, 30.6, 28.7, 22.7, 22.1, 21.2, 20.1, 19.6, 17.6, 16.5, 15.6, 13.7 ppm; HRMS (ESI – TOF) *m/Z*: $[M+H]^+$, calculated for $C_{34}H_{45}IN_3O_7^+$ 734.2297; found 734.2295.

***Z*-Isomer** (**35**): m.p. 132 °C; TLC R_f = 0.25 (hexanes/EtOAc = 3:7); $[\alpha]_D^{24}$ = +1.4 (c = 0.1, $CHCl_3$/MeOH = 1:1); IR (ATR): $\tilde{\nu}$ = 3031 (w), 2970 (w), 2653 (w), 2421 (w), 2373 (w), 2347 (w), 2321 (w), 2259 (w), 2220 (w), 1986 (w), 1868 (w), 1734 (m), 1654 (m), 1541 (m), 1508 (m), 1457 (m), 1419 (m), 1374 (m), 1272 (w), 1025 (w), 830 (w), 800 (w), 763 (w), 720 (w), 669 (m) cm^{-1}; ^{1}H NMR (600 MHz, DMSO-d_6, 297 K): δ = 10.06 (s, 1H), 9.30 (s, 1H), 8.27 (d, *J* = 8.8 Hz, 1H), 7.98 (d, *J* = 7.4 Hz, 1H), 7.48 (d, *J* = 1.9 Hz, 1H), 7.10–6.95 (m, 4H), 6.76–6.62 (m, 4H), 5.24 (dd, *J* = 10.9, 5.1 Hz, 1H), 5.15 (d, *J* = 6.3 Hz, 1H), 5.02 (d, *J* = 9.1 Hz, 1H), 4.59–4.49 (m, 1H), 4.46–4.35 (m, 1H), 2.97 (s, 3H), 2.82 (d, *J* = 9.2 Hz, 4H), 2.63–2.54 (m, 1H), 2.42–2.26 (m, 3H), 1.88 (d, *J* = 7.1 Hz, 1H), 1.66 (s, 3H), 1.56–1.46 (m, 2H), 1.40 – 1.22 (m, 3H), 1.13–1.04 (m, 1H), 1.01 (d, *J* = 6.2 Hz, 3H), 0.91 (d, *J* = 6.8 Hz, 3H), 0.83 (dd, *J* = 9.8, 6.9 Hz, 6H) ppm; ^{13}C{^{1}H} NMR (125 MHz, DMSO-d_6, 297 K): δ = 174.8, 173.3, 170.4, 169.4, 161.2, 156.8, 155.5, 139.1, 133.4, 132.7, 131.2, 130.6, 130.5, 127.7, 115.4, 115.4, 114.9, 84.6, 71.8, 60.6, 58.9, 56.2, 54.2, 52.9, 48.6, 45.3, 44.8, 44.3, 41.7, 37.2, 36.3, 33.2, 30.9, 29.5, 23.1, 22.6, 22.4, 20.0, 17.9, 17.7 ppm; HRMS (ESI – TOF) *m/Z*: $[M+H]^+$, calculated for $C_{34}H_{45}IN_3O_7^+$ 734.2297; found 734.2301.

Desmethyl geodiamolide H analogue 36

Final deprotection was conducted with 18 mg of compound **31**. Purification by using prep. HPLC gave 11 mg of geodiamolide analogue **36** (74% yield) as a colourless amorphous resin. TLC R_f = 0.20 (hexanes/EtOAc = 3:7); $[\alpha]_D^{24}$ = +22.4 (c = 0.1, $CHCl_3$/MeOH =

1:1); IR (ATR): $\tilde{\nu}$ = 2930.4 (w), 2581.3 (w), 2453.5 (w), 2376.8 (w), 2313 (w), 2028.6 (w), 1920 (w), 1869.1 (w), 1718.7 (m), 1635.6 (m), 1508.7 (m), 1416.8 (m), 1373.8 (m), 1216.8 (m), 1096 (m), 1036.2 (m), 954.48 (w), 828.95 (m), 731.79 (w), 668.48 (m) cm^{-1}; ^1H NMR (400 MHz, DMSO-d_6, 297 K): δ = 9.56 (m, *1*H), 8.95 (m, 1H); 8.56 (d, J = 8.9 Hz, 1H), 7.79 (d, J = 8.2 Hz, 1H), 7.10 (dd, J = 8.7, 2.2 Hz, 2H), 6.99 (d, J = 8.4 Hz, 2H), 6.69 (d, J = 8.5 Hz, 2H), 6.64–6.56 (m, 2H), 5.41 (dd, J = 11.6, 4.9 Hz, 1H), 5.15 (d, J = 8.5 Hz, 1H), 4.94 (t, J = 6.3 Hz, 1H), 4.78–4.53 (m, 2H), 2.98 (d, J = 4.9 Hz, 3H), 2.92–2.54 (m, 5H), 2.25–2.08 (m, 1H), 1.94 – 1.66 (m, 3H), 1.56–1.48 (m, 4H), 1.46–1.31 (m, 1H), 1.17 (d, J = 6.3 Hz, 3H), 0.94 (d, J = 6.8 Hz, 3H), 0.60 (dd, J = 11.6, 4.4 Hz, 3H) ppm; $^{13}C\{^1H\}$ NMR (101 MHz, DMSO-d_6, 297 K): δ = 174.5, 173.7, 170.7, 170.0, 170.0, 156.8, 155.5, 138.8, 133.4, 130.5, 130.2, 127.5, 127.4, 123.6, 115.6, 114.8, 84.7, 71.4, 55.5, 55.4, 49.6, 49.1, 44.1, 43.2, 42.4, 37.9, 35.3, 34.1, 31.2, 24.2, 19.9, 19.9, 19.7, 17.9, 17.4 ppm; HRMS (ESI – TOF) *m/Z*: $[M+H]^+$, calculated for $C_{33}H_{43}IN_3O_7^+$ 720.2140; found 720.2139.

Deposition Numbers 1938340 (for **S3c**) and 1938341 (for **16c**) contain the supplementary crystallographic data for this paper. These data are provided free of charge by the joint Cambridge Crystallographic Data Centre and Fachinformationszentrum Karlsruhe Access Structures service.

Acknowledgements

V.N. was recipient of a DAAD predoctoral fellowship. P.S. and H.-D.A. received funding from the Deutsche Forschungsgemeinschaft (German Research Foundation) collaborative research center SFB1127/2 ChemBioSys-Project ID 239748522. P.S. is grateful for financial support from the Leibniz Association and the Werner Siemens-Stiftung. This work benefitted in part from an equipment grant of the DFG (INST 275/33-1-1 FUGG) that is kindly acknowledged. Open access funding enabled and organized by Projekt DEAL.

Conflict of Interest

The authors declare no conflict of interest.

Keywords: Actin · antitumor agents · natural products · structure-activity relationship · total synthesis

[1] W. F. Tinto, A. J. Lough, S. McLean, W. F. Reynolds, M. Yu, W. R. Chan, *Tetrahedron* **1998**, *54*, 4451–4458.
[2] F. Gala, M. V. D'Auria, S. De Marino, V. Sepe, F. Zollo, C. D. Smith, S. N. Keller, A. Zampella, *Tetrahedron* **2009**, *65*, 51–56.
[3] S. Rachid, D. Krug, B. Kunze, I. Kochems, M. Scharfe, T. M. Zabriskie, H. Blocker, R. Müller, *Chem. Biol.* **2006**, *13*, 667–681.
[4] K. Gemperlein, N. Zaburannyi, R. Garcia, J. J. La Clair, R. Müller, *Mar. Drugs* **2018**, *16*, 314.
[5] T. D. Pollard, J. A. Cooper, *Science* **2009**, *326*, 1208–1212.
[6] C. Tanaka, J. Tanaka, R. F. Bolland, G. Marriott, T. Higa, *Tetrahedron* **2006**, *62*, 3536–3542.
[7] J. Sorres, M. T. Martin, S. Petek, H. Levaique, T. Cresteil, S. Ramos, O. Thoison, C. Debitus, A. Al-Mourabit, *J. Nat. Prod.* **2012**, *75*, 759–763.
[8] M. V. D'Auria, L. Gomez Paloma, L. Minale, A. Zampella, C. Debitus, J. Perez, *J. Nat. Prod.* **1995**, *58*, 121–123.
[9] T. Iizuka, R. Fudou, Y. Jojima, S. Ogawa, S. Yamanaka, Y. Inukai, M. Ojika, *J. Antibiot.* **2006**, *59*, 385–391.
[10] R. Tannert, L. G. Milroy, B. Ellinger, T. S. Hu, H. D. Arndt, H. Waldmann, *J. Am. Chem. Soc.* **2010**, *132*, 3063–3077.
[11] M. Verderame, D. Alcorta, M. Egnor, K. Smith, R. Pollack, *Proc. Natl. Acad. Sci. USA* **1980**, *77*, 6624–6628.
[12] F. Merino, S. Pospich, J. Funk, T. Wagner, F. Küllmer, H. D. Arndt, P. Bieling, S. Raunser, *Nat. Struct. Mol. Biol.* **2018**, *25*, 528–537.
[13] G. Lukinavicius, L. Reymond, E. D'Este, A. Masharina, F. Gottfert, H. Ta, A. Güther, M. Fournier, S. Rizzo, H. Waldmann, C. Blaukopf, C. Sommer, D. W. Gerlich, H. D. Arndt, S. W. Hell, K. Johnsson, *Nat. Methods* **2014**, *11*, 731–733.
[14] V. N. Belov, S. Stoldt, F. Rüttger, M. John, J. Seikowski, J. Schimpfhauser, S. W. Hell, *J. Org. Chem.* **2020**, *85*, 7267–7275.
[15] S. Wang, A. H. Crevenna, I. Ugur, A. Marion, I. Antes, U. Kazmaier, M. Hoyer, D. C. Lamb, F. Gegenfurtner, Z. Kliesmete, C. Ziegenhain, W. Enard, A. Vollmar, S. Zahler, *Sci. Rep.* **2019**, *9*, 9731.
[16] D. Becker, U. Kazmaier, *Eur. J. Org. Chem.* **2015**, 2591–2602.
[17] V. Nasufovic, P. Then, F. Dröge, M. Duong, C. Kaether, B. Dietzek, R. Heintzmann, H. D. Arndt, *Org. Biomol. Chem.* **2021**, *19*, 574–578.
[18] A. Gandalovicova, D. Rosel, M. Fernandes, P. Vesely, P. Heneberg, V. Cermak, L. Petruzelka, S. Kumar, V. Sanz-Moreno, J. Brabek, *Trends Cancer* **2017**, *3*, 391–406.
[19] K. A. Whitehead, R. Langer, D. G. Anderson, *Nat. Rev. Drug Discovery* **2009**, *8*, 129–138.
[20] E. L. Sievers, P. D. Senter, *Annu. Rev. Med.* **2013**, *64*, 15–29.
[21] M. Borowiak, F. Küllmer, F. Gegenfurtner, S. Peil, V. Nasufovic, S. Zahler, O. Thorn-Seshold, D. Trauner, H. D. Arndt, *J. Am. Chem. Soc.* **2020**, *142*, 9240–9249.
[22] J. D. White, J. C. Amedio, *J. Org. Chem.* **1989**, *54*, 736–738.
[23] Y. Hirai, K. Yokota, H. Sakai, T. Yamazaki, T. Momose, *Heterocycles* **1989**, *29*, 1865–1869.
[24] A. V. R. Rao, M. K. Gurjar, B. Rao Nallaganchu, A. Bhandari, *Tetrahedron Lett.* **1993**, *34*, 7085–7088.
[25] M. Rangel, M. P. Prado, K. Konno, H. Naoki, J. C. Freitas, G. M. Machado-Santelli, *Peptides* **2006**, *27*, 2047–2057.
[26] V. M. Freitas, M. Rangel, L. F. Bisson, R. G. Jaeger, G. M. Machado-Santelli, *J. Cell. Physiol.* **2008**, *216*, 583–594.
[27] F. Gala, M. V. D'Auria, S. De Marino, V. Sepe, F. Zollo, C. D. Smith, J. E. Copper, A. Zampella, *Tetrahedron* **2008**, *64*, 7127–7130.
[28] H. Waldmann, T. S. Hu, S. Renner, S. Menninger, R. Tannert, T. Oda, H. D. Arndt, *Angew. Chem. Int. Ed.* **2008**, *47*, 6473–6477; *Angew. Chem.* **2008**, *120*, 6573–6577.
[29] H. Waldmann, T.-S. Hu, S. Renner, S. Menninger, R. Tannert, T. Oda, H.-D. Arndt, *Angew. Chem.* **2008**, *120*, 6573–6577; *Angew. Chem. Int. Ed.* **2008**, *47*, 6473–6477.
[30] T. Hintermann, D. Seebach, *Helv. Chim. Acta* **1998**, *81*, 2093–2126.
[31] H. M. Eng, D. C. Myles, *Tetrahedron Lett.* **1999**, *40*, 2279–2282.
[32] H. M. Eng, D. C. Myles, *Tetrahedron Lett.* **1999**, *40*, 2275–2278.
[33] D. A. Evans, M. D. Ennis, D. J. Mathre, *J. Am. Chem. Soc.* **1982**, *104*, 1737–1739.
[34] A. P. Pulis, D. J. Blair, E. Torres, V. K. Aggarwal, *J. Am. Chem. Soc.* **2013**, *135*, 16054–16057.
[35] A. Schulze, A. Giannis, *Adv. Synth. Catal.* **2004**, *346*, 252–256.
[36] N. Wang, R. Liu, Q. Xu, X. Liang, *Chem. Lett.* **2006**, *35*, 566–567.
[37] J. Chiarello, M. M. Joullie, *Synth. Commun.* **1988**, *18*, 2211–2223.
[38] A. El-Faham, F. Albericio, *J. Pept. Sci.* **2010**, *16*, 6–9.
[39] R. Subiros-Funosas, L. Nieto-Rodriguez, K. J. Jensen, F. Albericio, *J. Pept. Sci.* **2013**, *19*, 408–414.
[40] J. H. Lang, T. Lindel, *Beilstein J. Org. Chem.* **2019**, *15*, 577–583.
[41] J.-d. A. K. Twibanire, T. B. Grindley, *Org. Lett.* **2011**, *13*, 2988–2991.
[42] B. Neises, W. Steglich, *Angew. Chem. Int. Ed.* **1978**, *17*, 522–524; *Angew. Chem.* **1978**, *90*, 556–557.
[43] B. Neises, W. Steglich, *Angew. Chem.* **1978**, *90*, 556–557; *Angew. Chem. Int. Ed.* **1978**, *17*, 522–524.
[44] M. Pittelkow, F. S. Kamounah, U. Boas, B. Pedersen, J. B. Christensen, *Synthesis* **2004**, 2485–2492.
[45] L. Ghosez, I. George-Koch, L. Patiny, M. Houtekie, P. Bovy, P. Nshimyumukiza, T. Phan, *Tetrahedron* **1998**, *54*, 9207–9222.
[46] E. Harth-Fritschy, D. Cantacuzene, *J. Pept. Res.* **1997**, *50*, 415–420.
[47] I. Dhimitruka, J. Santalucia, Jr., *Org. Lett.* **2006**, *8*, 47–50.
[48] I. Shiina, M. Kubota, H. Oshiumi, M. Hashizume, *J. Org. Chem.* **2004**, *69*, 1822–1830.
[49] R. Tannert, T. S. Hu, H. D. Arndt, H. Waldmann, *Chem. Commun.* **2009**, 1493–1495.
[50] S. Monfette, D. E. Fogg, *Chem. Rev.* **2009**, *109*, 3783–3816.

[51] A. K. Chatterjee, T. L. Choi, D. P. Sanders, R. H. Grubbs, *J. Am. Chem. Soc.* **2003**, *125*, 11360–11370.
[52] J. Engel, W. Smit, M. Foscato, G. Occhipinti, K. W. Tornroos, V. R. Jensen, *J. Am. Chem. Soc.* **2017**, *139*, 16609–16619.
[53] B. Schmidt, *Eur. J. Org. Chem.* **2004**, *2004*, 1865–1880.
[54] S. H. Hong, D. P. Sanders, C. W. Lee, R. H. Grubbs, *J. Am. Chem. Soc.* **2005**, *127*, 17160–17161.
[55] S. Schieferdecker, S. König, C. Weigel, H.-M. Dahse, O. Werz, M. Nett, *Chem. Eur. J.* **2014**, *20*, 15933–15940.
[56] H. D. Arndt, S. Rizzo, C. Nöcker, V. N. Wakchaure, L. G. Milroy, V. Bieker, A. Calderon, T. T. Tran, S. Brand, L. Dehmelt, H. Waldmann, *Chem. Eur. J.* **2015**, *21*, 5311–5316.
[57] T. Rezai, J. E. Bock, M. V. Zhou, C. Kalyanaraman, R. S. Lokey, M. P. Jacobson, *J. Am. Chem. Soc.* **2006**, *128*, 14073–14080.
[58] R. A. Friesner, R. B. Murphy, M. P. Repasky, L. L. Frye, J. R. Greenwood, T. A. Halgren, P. C. Sanschagrin, D. T. Mainz, *J. Med. Chem.* **2006**, *49*, 6177–6196.
[59] S. Pospich, F. Merino, S. Raunser, *Structure* **2020**, *28*, 437–449.
[60] S. Genheden, U. Ryde, *Expert Opin. Drug Discovery* **2015**, *10*, 449–461.
[61] E. Wang, H. Sun, J. Wang, Z. Wang, H. Liu, J. Z. H. Zhang, T. Hou, *Chem. Rev.* **2019**, *119*, 9478–9508.
[62] S. Pospich, E. P. Kumpula, J. von der Ecken, J. Vahokoski, I. Kursula, S. Raunser, *Proc. Natl. Acad. Sci. USA* **2017**, *114*, 10636–10641.
[63] F. Merino, S. Pospich, S. Raunser, *Semin. Cell Dev. Biol.* **2020**, *102*, 51–64.
[64] S. Pospich, F. Küllmer, V. Nasufovic, J. Funk, A. Belyy, P. Bieling, H. D. Arndt, S. Raunser, *Angew. Chem. Int. Ed.* **2021**, *60*, 8678–8682.
[65] S. Pospich, F. Küllmer, V. Nasufovic, J. Funk, A. Belyy, P. Bieling, H. D. Arndt, S. Raunser, *Angew. Chem.* **2021**, *133*, 8760–8764.
[66] J. C. Ma, D. A. Dougherty, *Chem. Rev.* **1997**, *97*, 1303–1324.
[67] H. Lin, J. l. Luengo, *Bioorg. Med. Chem. Lett.* **2020**, *30*, 127442.
[68] D. Eisenberg, E. Schwarz, M. Komaromy, R. Wall, *J. Mol. Biol.* **1984**, *179*, 125–142.
[69] P. Thiel, M. Kaiser, C. Ottmann, *Angew. Chem. Int. Ed.* **2012**, *51*, 2012–2018; *Angew. Chem.* **2012**, *124*, 2052–2059.
[70] P. Thiel, M. Kaiser, C. Ottmann, *Angew. Chem.* **2012**, *124*, 2052–2059; *Angew. Chem. Int. Ed.* **2012**, *51*, 2012–2018.
[71] S. L. Schreiber, *Cell* **2021**, *184*, 3–9.

Manuscript received: April 18, 2021
Accepted manuscript online: May 25, 2021
Version of record online: June 25, 2021

